ACS Partner Journal

CHEM & BIO ENGINEERING

pubs.acs.org/ChemBioEng

Article

Adsorptive Separation of Methylfuran and Dimethylfuran by a Robust Porous Organic Cage

Published as part of Chem & Bio Engineering virtual special issue "Advanced Separation Materials and Processes".

Fenglei Qiu,[#] Ning Xu,[#] Wenjing Wang, Kongzhao Su,[*] and Daqiang Yuan[*]

Cite This: *Chem Bio Eng.* 2024, 1, 171−178

Read Online

ACCESS | Metrics & More | Article Recommendations | Supporting Information

ABSTRACT: As vital raw materials in the chemical industry, 2-methylfuran (**MeF**) and 2,5-dimethylfuran (**DMeF**) are commonly produced as mixtures. The selective separation of **MeF** and **DMeF** is crucial yet challenging, with significant industrial and economic implications. This study presents an energy-efficient separation technique using a robust calix[4]resorcinarene-based supramolecular porous organic cage (POC), **CPOC-301**, to effectively capture **DMeF** from an equimolar **MeF**/**DMeF** mixture within 2 h, yielding 95.3% purity. The exceptional separation efficiency stems from the superior structural stability of **CPOC-301**, maintaining its initial porous crystalline structure during separation. Calculations show that **CPOC-301** forms more C−H···π hydrogen bonds with **DMeF** versus **MeF**, accounting for its **DMeF** selectivity. **CPOC-301** can be easily regenerated via heat under a vacuum and reused for over five adsorption−desorption cycles without significant performance loss. This work introduces an approach to separate similar organic molecules effectively using POC materials.

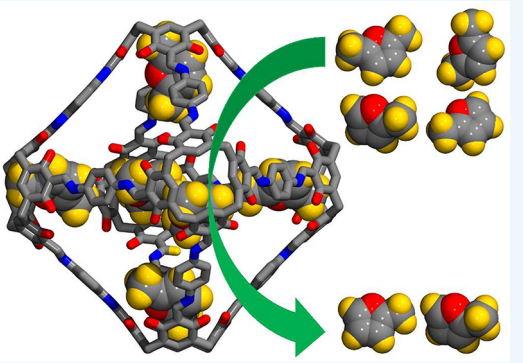

KEYWORDS: *porous organic cage (POC), calix[4]resorcinarene, organic vapor separation, furan derivatives, host−guest interaction*

1. INTRODUCTION

Efficiently separating important chemical raw materials is widely considered an extremely challenging task. In pharmaceutical production, 2-methylfuran (**MeF**) and 2,5-dimethylfuran (**DMeF**) are typical furan derivatives and are greatly valued.[1] These compounds possess versatile applications as essential feedstocks for producing various fine chemicals, including medicines, pesticides, and biofuels.[2−5] Due to the simultaneous formation of **MeF** and **DMeF** as the primary products during the dehydration and hydrogenolysis of fructose, a mixture containing both compounds unavoidably arises. An effective separation of the **MeF** and **DMeF** mixture is necessary to obtain high-purity chemicals. The separation methods, such as azeotropic and extractive distillation, generally involve high energy consumption and complex operational steps.[6,7] Furthermore, these traditional separation methods cannot efficiently separate **MeF** and **DMeF** due to their close boiling points and the potential formation of azeotropes. Consequently, an urgent need remains to develop efficient and energy-saving separation methods for **MeF** and **DMeF** mixtures, which poses a significant challenge.

Recently, the adsorptive separation technology based on porous materials has received escalating attention owing to the convenient operation process and low energy requirements.[8−13] By taking advantage of the differences in size, geometry, and physicochemical properties of **MeF** and **DMeF** molecules, many well-established porous framework materials, including metal-organic frameworks (MOFs), porous organic polymers (POPs), and covalent organic frameworks (COFs), have shown superiority in the separation processes of such type organic molecules with similar structures.[14−19] Nevertheless, the above-mentioned separation materials still have structural stability, processability, and economic scale limitations. Developing novel adsorbents with high stability and economic feasibility is imperative and desirable for the practical separation of **MeF** and **DMeF** mixtures. Apart from the above-mentioned framework materials, some recently reported discrete supramolecules also show great potential in **MeF**/**DMeF** separation.[20−25] For instance, Huang's group has reported a novel strategy for separating the **MeF** and **DMeF** mixtures with remarkable selectivity and high recyclability by

Received: November 28, 2023
Revised: January 20, 2024
Accepted: January 21, 2024
Published: February 2, 2024

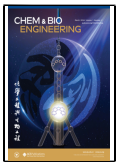

https://doi.org/10.1021/cbe.3c00099
Chem Bio Eng. 2024, 1, 171−178

nonporous adaptive crystals (NACs) of supramolecular perbromoethylated pillar[5]arene and perethylated pillar[6]-arene.[26]

Porous organic cages (POCs) represent a novel category of porous organic molecular materials characterized by covalently bonded discrete supramolecular molecules with well-defined internal cavities.[27−32] The distinct and discrete nature of POCs bestows them notable advantages, such as solution processing, easy regeneration, and large-scale production.[33−39] These emerging molecular hosts and functional materials have garnered significant attention and exhibited flourishing development trends in various applications, including gas adsorption, molecular recognition, sensing, encapsulation, and catalyst supports.[40−51] Leveraging the hollow cavity with multiple pore windows, POCs enable facile host−guest recognition and selective adsorptive separation.[52−56] Additionally, the strategic incorporation of functional building blocks into the cage framework enhances the host−guest interactions, thereby facilitating the precise separation of specific compounds.[57,58] POCs have achieved significant progress in gas separation, but their exploration of liquid organic molecules remains limited and warrants further investigation. To our best knowledge, the utilization of POC adsorbents in separating liquid organic molecules has primarily been limited to mixtures such as mesitylene/4-ethyltoluene,[59] cyclohexane/benzene,[60] toluene/methylcyclohexane,[55] and xylene isomers.[61] Consequently, significant opportunities remain for the application of POCs in the separation of liquid organic molecules possessing similar structural characteristics.

As a member of calixarenes, calix[4]resorcinarene (C4RA) features an intrinsic electron-rich π cavity and eight polar upper-rim phenolic groups, which can encapsulate a wide variety of guests through multiple intermolecular interactions.[62] Our group has been developing new C4RA-based POCs and their potential applications in energy and the environment. Recently, our group employed the cavitand-shaped tetraformylresorcin[4]arene (C4RACHO) scaffold and different diamine and dihydrazide linkers to construct a series of POCs with diverse self-assembly topologies.[63,64] Some of the synthesized POCs can function as robust absorbents for gas molecules, water pollutants, and C_{60}.[65−70] However, such C4RA-based POCs have never been used to achieve the effective absorption and separation of organic molecules with similar structures. Herein, the porous [6+12] octahedral calix[4]resorcinarene-based POC (**CPOC-301**) was utilized as a highly efficient separation material to selectively separate **DMeF** from a mixture of **MeF** and **DMeF**, which also presents the first example of a POC adsorbent for **MeF**/**DMeF** separation. Attributed to the highly stable porous crystalline structure with large accessible channels during the separation process, **CPOC-301** exhibits excellent separation ability for **DMeF** in the vapor of **MeF**/**DMeF** (50:50) mixture, resulting in **DMeF** with a purity of 95.3% within 2 h. Theoretical calculations suggest that more multiple C−H···π hydrogen bonds between **CPOC-301** and **DMeF** account for the excellent selectivity toward **DMeF** in comparison with **MeF**.

2. EXPERIMENTAL SECTION

2.1. Chemicals and Materials. Except for C4RACHO, prepared according to the reported literature method,[71] other chemicals in this work were commercially available and used as received without further purification. Specifically, *p*-phenylenediamine (PDA), **MeF**, and **DMeF** were purchased from Shanghai Titan Scientific Co., Ltd. (Shanghai, China), while methanol (MeOH), chloroform ($CHCl_3$), and nitrobenzene ($PhNO_2$) were obtained from Sinopharm Chemical Reagent Co., Ltd. (Ningbo, China).

2.2. Synthesis of CPOC-301. This cage was synthesized using a procedure previously published by our research group,[64] with slight modifications made to enhance the synthetic yield. C4RACHO (0.10 mmol, 82 mg) and PDA (0.2 mmol, 21.5 mg) were added to $CHCl_3$ (6 mL) and $PhNO_2$ (1.5 mL). The mixture was sealed in a 20 mL pressure vial, and the vial was then put in an oil bath heated to 65 °C with stirring for 24 h. After removing the glass vial from the oil bath and allowing it to cool to room temperature, slow vapor diffusion of MeOH into the above-mentioned mixture was conducted for 3 days. Red block single crystals of **CPOC-301** were filtrated and washed with methanol three times. The separated crystals were further immersed and exchanged 6 times every 24 h in methanol before activating at 100 °C under a high vacuum for 12 h to afford **CPOC-301** with a yield of about 83%. ^{1}H NMR (400 MHz, $CDCl_3$, 298 K): δ 16.21 (s, 24H), 10.34 (s, 48H). 9.18 (s, 24H), 7.40 (s, 24H), 7.37 (s, 48H), 4.63 (t, 24H), 2.10 (t, 48H), 1.55 (m, 24H), 1.03 (d, 144H) ppm. Upon mounting several of the obtained crystals, it was observed that they had the same unit cell parameters as those of **CPOC-301**. Moreover, the powder X-ray diffraction (PXRD) pattern of the obtained activated sample was consistent with the simulated PXRD spectrum pattern. Both the above test results revealed the uniformity of the sample.

2.3. General Procedure for Uptake from MeF and DMeF by CPOC-301. For each vapor-phase mixture experiment, an open 5.00 mL vial containing 20.00 mg of guest-free **CPOC-301** adsorbent was placed in a sealed 20.00 mL vial containing 1.00 mL of a 50:50 v/v **MeF** and **DMeF** mixture. After measurements, the crystals were heated in a vacuum drying oven at 40 °C for 30 min to remove the surface-physically adsorbed vapor. The treated **CPOC-301** was immersed in methanol to release the adsorbed guest molecules fully. The methanol solution was collected and tested by gas chromatography (GC).

2.4. Characterizations. PXRD patterns were measured over a desktop X-ray diffractometer (Rigaku Mini 600) with Cu Kα radiation source (λ = 0.154 Å) with a 2θ degree from 4° to 40°. Fourier-transformed infrared (FT-IR) spectrum was collected by a VERTEX70 FT-IR spectrometer with a wavenumber from 400 to 4000 cm^{-1} by dispersing the sample in KBr disks. ^{1}H NMR spectra were conducted on a Bruker Avance II 400 WB 400 MHz spectrometer equipped with a 4 mm double-resonance MAS probe and a spinning frequency of 8 kHz. GC measurements were performed using a Shimadzu GC-2010 gas chromatography instrument equipped with an MXT-WAX column (60 m × 0.53 mm × 1.50 μm) with the following parameters. Specifically, the oven is programmed from 50 °C and heated up to 280 °C at a rate of 5 °C min^{-1}, the samples were injected in a shunt mode (20:1), the helium (carrier gas) flow rate is 4.16 mL min^{-1}, the total running time is 35 min, and the nitrogen, air, and recharge flow rates were 30, 400, and 35 mL/min, respectively.

2.5. Computational Method. The binding sites for **MeF** and **DMeF** in **CPOC-301** were determined through classical simulated annealing (SA) calculation.[72] The single X-ray crystallographic structure for **CPOC-301** was used as a starting point to perform parametrizations and simulations. The resultant structures were subject to geometry optimization,

https://doi.org/10.1021/cbe.3c00099
Chem Bio Eng. 2024, 1, 171−178

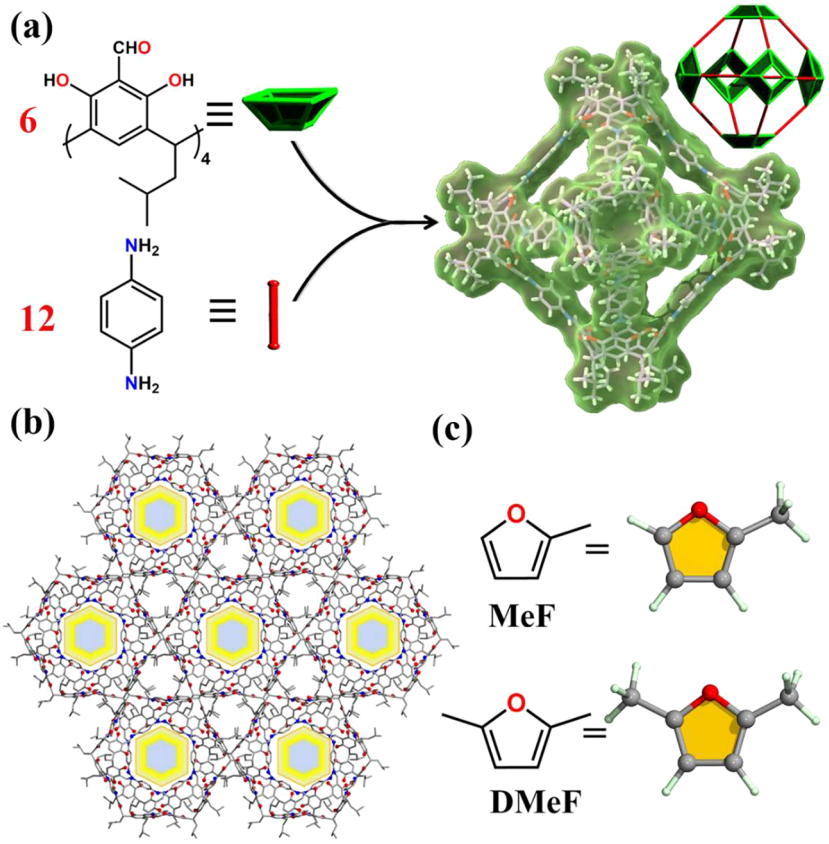

Figure 1. (a) Design and synthesis of [6+12] calix[4]resorcinarene-based **CPOC-301** and structural representation for **CPOC-301** obtained from single-crystal X-ray diffraction. (b) Molecular packing of **CPOC-301** in the solid state viewed from the [001] direction. Hydrogen atoms are omitted for clarity. (c) Chemical structures of **MeF** and **DMeF**. Carbon is gray, oxygen is red, hydrogen is light green, and nitrogen is blue.

implemented with the CP2K code with the tight-binding method GFN-xTB.[73−75] In all calculations, Grimme's DFT-D3 dispersion correction was applied.[76] A 1.0×10^{-6} hartree convergence threshold was used for all self-consistent-field (SCF) calculations. The structural optimizations were considered converged if the maximum force on all atoms falls below 4.5×10^{-4} hartree bohr^{-1}. The binding energy can be obtained from the formula below:

$$E_{binding} = E_{system} - E_{poc} - E_{adsorbate}$$

where E_{system} and E_{poc} were the total energies of the **CPOC-301** with and without adsorbate, and $E_{adsorbate}$ was the energy of the adsorbate (**MeF** and **DMeF**).

3. RESULTS AND DISCUSSION

3.1. Synthesis and Characterizations of CPOC-301. As shown in Figure 1a, **CPOC-301** was synthesized by utilizing [6+12] imine condensation reactions, where 1 equiv of C4RACHO was combined with 2 equiv of PDA under mild conditions, as previously described.[64] Analysis using single-crystal X-ray diffraction revealed that **CPOC-301** possesses a truncated octahedron structure. It consists of eight trigonal ports with an edge length of approximately 12 Å, a large cavity with an inner diameter of 16.8 Å, and a volume of 4270 Å^3. The solid-state packing arrangement of **CPOC-301** indicates the presence of a one-dimensional channel with a diameter of approximately 7 Å when viewed from the [001] direction (Figure 1b). Moreover, previous reports have shown that **CPOC-301** exhibits high specific surface areas with Brunauer−Emmett−Teller (BET) surface areas up to ∼2000 m^2 g^{-1}, with a pore-size distribution value of ∼1.65 nm (Figure S1), remarkable structural stability from keto-enamine tautomerization behavior (Figure S2), and retention solid-state packing after desolvation (Figure S3), making it highly promising for investigating its adsorptive separation performance for the **MeF**/**DMeF** mixture (Figure 1c).

3.2. Single-Component Vapor Adsorption Experiments. To evaluate the adsorptive capacity of **CPOC-301** toward **MeF** and **DMeF**, single-component solid−vapor sorption experiments were conducted using activated samples of **CPOC-301**. As shown in Figure 2a, it took approximately 2 h for **CPOC-301** to reach saturation adsorption points for both **MeF** and **DMeF** vapors. The final adsorption ratios were nearly ten **MeF** molecules per cage and 12 **DMeF** molecules per cage, respectively (Figures S4 and S5). Notably, the adsorption capacity and rate of **CPOC-301** were significantly higher than those of the previously reported pillar[*n*]arene-based NAC materials.[26] This suggests that **CPOC-301** may have advantages in separating mixtures of **MeF** and **DMeF**. It is worth mentioning that the adsorption of **DMeF** was faster than that of **MeF**, indicating the kinetic selectivity of **CPOC-301** toward **DMeF**. The higher adsorption molar ratio of **DMeF** to the host indicates that the **DMeF** vapor preferably occupies the cavity of **CPOC-301**, which can be attributed to stronger host−guest interactions. Moreover, it is essential to note that the saturation point of **CPOC-301** for the **MeF** and **DMeF** mixture was achieved in less than 2 h, significantly faster than the reported pillar[*n*]arene-based NAC materials which typically require approximately 8−12 h under the same

https://doi.org/10.1021/cbe.3c00099
Chem Bio Eng. 2024, 1, 171−178

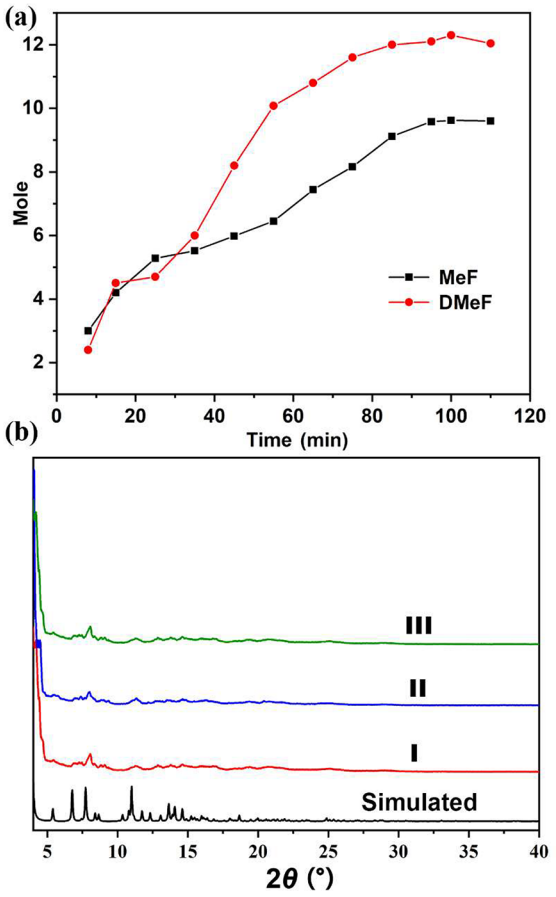

Figure 2. (a) Time-dependent solid−vapor adsorption plots of **CPOC-301** and (b) PXRD patterns of **CPOC-301**: (I) activated crystals of the host; (II) after adsorption of **DMeF** vapor; (III) after adsorption of **MeF** vapor.

conditions. This can be attributed to the presence of one-dimensional channels in solid-state **CPOC-301**, which facilitate the diffusion of **MeF** and **DMeF** vapors, as the PXRD patterns of **CPOC-301** after absorbing guest vapors showed minor differences compared to the original patterns (Figure 2b), indicating that **CPOC-301** maintains its initial crystalline structure during the adsorption processes. To further confirm the effect of the internal cavity of **CPOC-301** on the vapor adsorption of **MeF** and **DMeF**, solid−vapor sorption experiments were conducted with C4RACHO using the same procedure as that of **CPOC-301**. The results demonstrated that C4RACHO did not exhibit adsorption behavior for both **MeF** and **DMeF** vapors (Figure S6), thus providing evidence for the crucial role of the inner cavity.

3.3. Selective Separation of MeF/DMeF Mixtures and Recyclability Experiments. Considering the exceptional adsorption performance of **CPOC-301** and its kinetically selective adsorption behavior toward **DMeF**, it can be inferred that **CPOC-301** has a preference for adsorbing **DMeF** molecules, thus achieving effective separation of **MeF** and **DMeF** mixtures. To further evaluate the separation selectivity of **CPOC-301** for **MeF**/**DMeF** mixtures, we conducted a time-dependent adsorption experiment using an equimolar **MeF**/**DMeF** mixture. As anticipated, **CPOC-301** exhibited exclusive uptake of **DMeF**, adsorbing approximately 12 equiv of **DMeF** after saturation, while the adsorption of **MeF** was negligible (Figure 3a). The adsorption rate of **CPOC-301** for the **MeF**/

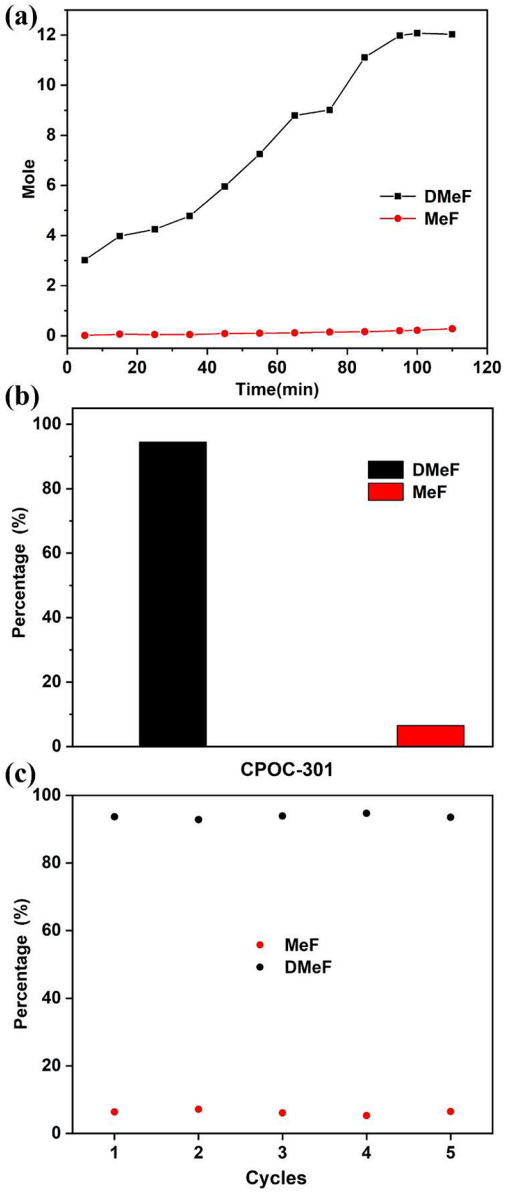

Figure 3. (a) Time-dependent solid−vapor adsorption plots of **CPOC-301**. (b) Relative amounts of **MeF** and **DMeF** adsorbed by **CPOC-301**. (c) Recycling tests of **CPOC-301** for the **MeF**/**DMeF** separation.

DMeF mixture vapor was not significantly different from that of the individual components. GC analysis confirmed that the vapor adsorbed by **CPOC-301** consisted of 95.3% **DMeF** (Figure 3b and Figure S7), thus substantiating the remarkable selectivity of **CPOC-301** for **DMeF**. Notably, the saturation point of **CPOC-301** for the **MeF**/**DMeF** mixture (<2 h) is much less than the reported pillar[*n*]arene-based NAC materials (~10 h),[26] which is mainly due to the one-dimensional guest-accessible channels in solid-state **CPOC-301**, as mentioned previously. The PXRD patterns of **CPOC-301** were compared before and after exposure to **MeF**/**DMeF** mixture vapor. The comparison showed that the solid-state crystal packing of **CPOC-301** remained unchanged after the selective capture of **DMeF** from the mixture (Figure S8). Additionally, **CPOC-301** prefers adsorbing **DMeF** guests, unlike the reported pillar[*n*]arene-based NAC materials, which tend to adsorb **MeF** guests. Hence, this study presents a

https://doi.org/10.1021/cbe.3c00099
Chem Bio Eng. 2024, 1, 171−178

potential alternative for efficiently separating **MeF**/**DMeF** mixtures. In practical industrial applications, the reusability of adsorbents is of significant importance. Cyclic adsorption experiments were conducted to evaluate the recycling capability of **CPOC-301**. After the adsorption of the **MeF**/**DMeF** mixture, **CPOC-301** could be easily regenerated by heating the guest-loaded samples under a vacuum at 60 °C. Analysis using ^{1}H NMR spectroscopy confirmed the complete release of the adsorbed **MeF** and **DMeF** molecules (Figure S9). PXRD analysis revealed that the crystallinity of the regenerated samples remained consistent with that of the activated **CPOC-301** crystals (Figure S10). Furthermore, the ^{1}H NMR spectrum and 77 K nitrogen gas adsorption isotherms of the regenerated **CPOC-301** exhibit similarities to those of the pristine **CPOC-301** (Figures S1 and S11). These results suggest that **CPOC-301** possesses excellent structural stability and high recyclability. Furthermore, the recycling experiments demonstrated that the recycled **CPOC-301** samples maintained their ability to separate the **MeF** and **DMeF** mixtures without any noticeable performance degradation for up to five adsorption−desorption cycles (Figure 3c).

3.4. Mechanism of Selective Separation. Modeling studies were conducted using the GFN1-xTB Semiempirical Extended Tight-Binding quantum chemistry methods implemented with the CP2K program to investigate the primary adsorption sites of the **CPOC-301** host with **DMeF** compared to **MeF** guests.[77,78] The initial cage hosts were optimized based on single-crystal data, and **DMeF** and **MeF** were then loaded into the cavities for further optimization. The lowest-energy binding configurations of the final structures of **CPOC-301** with the loaded organic molecules were calculated by using dispersion-corrected density functional theory (DFT-D) and are presented in Figure 4. For clarity, only one adsorption site is shown; the remaining five sites are identical. It was observed that the primary adsorption sites for **DMeF** guests were located in the C4RA cavities through multiple C−H···π and C−H···O interactions. **DMeF** exhibited seven C−H···π hydrogen bonds with distances ranging from 2.80 to 3.39 nm, and six C−H···O bonds with distances ranging from 2.56 to 3.86 nm, whereas **MeF** showed four C−H···π hydrogen bonds with distances ranging from 2.86 to 4.0 nm and five C−H···O bonds with distances ranging from 2.49 to 3.62 nm. The stronger host−guest interactions between **DMeF** and C4RA compared to MeF are evident due to the additional methyl group in **DMeF**, which provides more H atoms and a better steric fit to the C4RA cavities compared to those of the planar **MeF** molecule. Furthermore, the calculated static binding energies for **DMeF** and **MeF** were −67.8 and −58.3 kJ mol^{-1} for **CPOC-301**, respectively, confirming the stronger host−guest interactions between **DMeF** and C4RA.

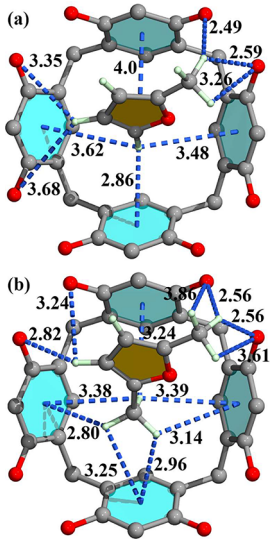

Figure 4. (a) **MeF** and (b) **DMeF** adsorption sites in **CPOC-301**. Carbon is gray, oxygen is red, and hydrogen is light green. Dashed bonds highlight C−H··· π interactions, and the unit for the distances of the dashed bonds is nm.

FT-IR spectral analysis further supported the host−guest interaction between **CPOC-301** and **DMeF**. The FT-IR spectra of DMeF-loaded **CPOC-301** exhibited significant differences from the original **CPOC-301** and **DMeF** characteristic peaks (Figure S12). Specifically, an additional infrared spectral absorption peak at approximately 2765 cm^{-1} was observed in the DMeF-loaded **CPOC-301** sample, which can be attributed to the C−H···O interaction between **DMeF** and the −OH group of **CPOC-301**. Additionally, the characteristic peaks of the C4RA at the benzene ring position of DMeF-loaded **CPOC-301**, observed at approximately 700 cm^{-1} in the FT-IR spectrum, displayed significant shifts compared to those of **CPOC-301** and **DMeF**. These shifts can be interpreted as resulting from the C−H···π interactions between the **DMeF** guest and the C4RA host.

4. CONCLUSIONS

In summary, we present the first example of a robust octahedral calix[4]resorcinarene-based POC, namely, **CPOC-301**, for effectively separating **MeF** and **DMeF** mixtures. By virtue of the inherent internal voids, **CPOC-301** can readily achieve the rapid adsorption of **MeF** and **DMeF** vapors until saturation. Taking advantage of the difference in host−guest interactions, **CPOC-301** allowed **DMeF** to be separated from an equimolar **MeF**/**DMeF** mixture through solid−vapor adsorption with 95.3% purity within 2 h. The outstanding sorting ability of **CPOC-301** toward **DMeF** originates from the more multiple C−H···π hydrogen bonds between **CPOC-301** and **DMeF** in comparison with **MeF**, as evidenced by theoretical calculations. Additionally, **CPOC-301** was highly recyclable and could be reused for at least five cycles without performance loss. The good structural stability, prominent separation efficiency, and excellent recycling performance enable **CPOC-301** to have great potential for industrial purification of **MeF** and **DMeF** mixtures. The findings hold promise for the application of POC materials in industrial processes, offering a reliable and efficient method of separating organic molecules for various chemical applications. Further works on separating chemically important feedstock, such as monochlorotoluene isomers, xylene isomers, and haloalkene isomers, are ongoing.

■ ASSOCIATED CONTENT

Supporting Information

The Supporting Information is available free of charge at https://pubs.acs.org/doi/10.1021/cbe.3c00099.

Additional N_2 gas sorption, ^{1}H NMR, PXRD, GC, and FT-IR spectra related to **CPOC-301** and regenerated **CPOC-301** (PDF)

https://doi.org/10.1021/cbe.3c00099
Chem Bio Eng. 2024, 1, 171−178

AUTHOR INFORMATION

Corresponding Authors

Kongzhao Su − *State Key Laboratory of Structural Chemistry, Fujian Institute of Research on the Structure of Matter, Chinese Academy of Sciences, Fuzhou 350002, China; University of Chinese Academy of Sciences, Beijing 100049, China;* orcid.org/0000-0001-9557-6982; Email: skz@fjirsm.ac.cn

Daqiang Yuan − *State Key Laboratory of Structural Chemistry, Fujian Institute of Research on the Structure of Matter, Chinese Academy of Sciences, Fuzhou 350002, China; University of Chinese Academy of Sciences, Beijing 100049, China;* orcid.org/0000-0003-4627-072X; Email: ydq@fjirsm.ac.cn

Authors

Fenglei Qiu − *State Key Laboratory of Structural Chemistry, Fujian Institute of Research on the Structure of Matter, Chinese Academy of Sciences, Fuzhou 350002, China; College of Chemistry, Fuzhou University, Fuzhou 350116, China*

Ning Xu − *State Key Laboratory of Structural Chemistry, Fujian Institute of Research on the Structure of Matter, Chinese Academy of Sciences, Fuzhou 350002, China; School of Chemical and Environmental Engineering, Anhui Polytechnic University, Wuhu 241000, China*

Wenjing Wang − *State Key Laboratory of Structural Chemistry, Fujian Institute of Research on the Structure of Matter, Chinese Academy of Sciences, Fuzhou 350002, China;* orcid.org/0000-0003-2139-1242

Complete contact information is available at: https://pubs.acs.org/10.1021/cbe.3c00099

Author Contributions

#F.Q. and N.X. contributed equally.

Notes

The authors declare no competing financial interest.

ACKNOWLEDGMENTS

This work was financially supported by the National Nature Science Foundation of China (22071244, 22275191), the Youth Innovation Promotion Association CAS (2022305), and the Natural Science Foundation of Fujian Province of China (2022J01503, 2020J05087).

REFERENCES

(1) Grela, M. A.; Amorebieta, V. T.; Colussi, A. J. Very low pressure pyrolysis of furan, 2-methylfuran and 2,5-dimethylfuran. The stability of the furan ring. *J. Phys. Chem. C* **1985**, *89* (1), 38.

(2) Wu, X.; Daniel, R.; Tian, G.; Xu, H.; Huang, Z.; Richardson, D. Dual-injection: The flexible, bi-fuel concept for spark-ignition engines fuelled with various gasoline and biofuel blends. *Appl. Energy* **2011**, *88* (7), 2305.

(3) Zhao, H.; Holladay, J. E.; Brown, H.; Zhang, Z. C. Metal chlorides in ionic liquid solvents convert sugars to 5-hydroxymethylfurfural. *Science* **2007**, *316* (5831), 1597.

(4) Hoang, A. T.; Olcer, A. I.; Nizetic, S. Prospective review on the application of biofuel 2,5-dimethylfuran to diesel engine. *J. Energy. Inst.* **2021**, *94*, 360.

(5) Tuan Hoang, A.; Viet Pham, V. 2-Methylfuran (MF) as a potential biofuel: A thorough review on the production pathway from biomass, combustion progress, and application in engines. *Renew. Sust. Energy Rev.* **2021**, *148*, 111265.

(6) Sholl, D. S.; Lively, R. P. Seven chemical separations to change the world. *Nature* **2016**, *532* (7600), 435.

(7) Shen, W.; Benyounes, H.; Gerbaud, V. Extractive distillation: recent advances in operation strategies. *Rev. Chem. Eng.* **2015**, *31* (1), 13.

(8) Wang, H.; Li, J. Microporous Metal-Organic Frameworks for Adsorptive Separation of C5-C6 Alkane Isomers. *Acc. Chem. Res.* **2019**, *52* (7), 1968.

(9) Wang, Z.; Zhang, S.; Chen, Y.; Zhang, Z.; Ma, S. Covalent organic frameworks for separation applications. *Chem. Soc. Rev.* **2020**, *49* (3), 708.

(10) Zhang, D.; Ronson, T. K.; Zou, Y.-Q.; Nitschke, J. R. Metal-organic cages for molecular separations. *Nat. Rev. Chem.* **2021**, *5* (3), 168.

(11) Barnett, B. R.; Gonzalez, M. I.; Long, J. R. Recent Progress Towards Light Hydrocarbon Separations Using Metal-Organic Frameworks. *Trends Chem.* **2019**, *1* (2), 159.

(12) Sun, M.; Liu, H.; Wang, X.; Yang, X.; Gao, F.; Xie, D.; Fan, W.; Han, Y.; Xu, B.; Sun, D. Metal-ion-tuned metal-organic frameworks for C_2H_2/CO_2 separation. *Chin. J. Struct. Chem.* **2023**, *42* (9), 100146.

(13) Yang, H.; Xue, L.; Yang, X.; Xu, H.; Gao, J. Advances in metal-organic frameworks for efficient separation and purification of natural gas. *Chin. J. Struct. Chem.* **2023**, *42* (2), 100034.

(14) Tan, H.; Chen, Q.; Chen, T.; Liu, H. Selective Adsorption and Separation of Xylene Isomers and Benzene/Cyclohexane with Microporous Organic Polymers POP-1. *ACS Appl. Mater. Interfaces* **2018**, *10* (38), 32717.

(15) Chiang, Y.; Bhattacharyya, S.; Jayachandrababu, K. C.; Lively, R. P.; Nair, S. Purification of 2,5-Dimethylfuran from n-Butanol Using Defect Engineered Metal Organic Frameworks. *ACS. Sustain. Chem. Eng.* **2018**, *6* (6), 7931.

(16) Gan, L.; Chidambaram, A.; Fonquernie, P. G.; Light, M. E.; Choquesillo-Lazarte, D.; Huang, H.; Solano, E.; Fraile, J.; Vinas, C.; Teixidor, F.; Navarro, J. A. R.; Stylianou, K. C.; Planas, J. G. A Highly Water-Stable meta-Carborane-Based Copper Metal-Organic Framework for Efficient High-Temperature Butanol Separation. *J. Am. Chem. Soc.* **2020**, *142* (18), 8299.

(17) Gonzalez, M. I.; Kapelewski, M. T.; Bloch, E. D.; Milner, P. J.; Reed, D. A.; Hudson, M. R.; Mason, J. A.; Barin, G.; Brown, C. M.; Long, J. R. Separation of Xylene Isomers through Multiple Metal Site Interactions in Metal-Organic Frameworks. *J. Am. Chem. Soc.* **2018**, *140* (9), 3412.

(18) Huang, J.; Han, X.; Yang, S.; Cao, Y.; Yuan, C.; Liu, Y.; Wang, J.; Cui, Y. Microporous 3D Covalent Organic Frameworks for Liquid Chromatographic Separation of Xylene Isomers and Ethylbenzene. *J. Am. Chem. Soc.* **2019**, *141* (22), 8996.

(19) Zhou, D.-D.; Chen, P.; Wang, C.; Wang, S.-S.; Du, Y.; Yan, H.; Ye, Z.-M.; He, C.-T.; Huang, R.-K.; Mo, Z.-W.; Huang, N.-Y.; Zhang, J.-P. Intermediate-sized molecular sieving of styrene from larger and smaller analogues. *Nat. Mater.* **2019**, *18* (9), 994.

(20) Jie, K.; Zhou, Y.; Li, E.; Huang, F. Nonporous Adaptive Crystals of Pillararenes. *Acc. Chem. Res.* **2018**, *51* (9), 2064.

(21) Wu, J.-R.; Yang, Y.-W. Synthetic Macrocycle-Based Nonporous Adaptive Crystals for Molecular Separation. *Angew. Chem. Int. Ed.* **2021**, *60* (4), 1690.

(22) Zhang, G.; Ding, Y.; Hashem, A.; Fakim, A.; Khashab, N. M. Xylene isomer separations by intrinsically porous molecular materials. *Cell Rep. Phys. Sci.* **2021**, *2* (6), 100470.

(23) Han, X.-N.; Han, Y.; Chen, C.-F. Recent advances in the synthesis and applications of macrocyclic arenes. *Chem. Soc. Rev.* **2023**, *52* (9), 3265.

(24) Song, N.; Kakuta, T.; Yamagishi, T.-a.; Yang, Y.-W.; Ogoshi, T. Molecular-Scale Porous Materials Based on Pillar n arenes. *Chem.* **2018**, *4* (9), 2029.

(25) Cai, Y.; Zhang, Z.; Ding, Y.; Hu, L.; Wang, J.; Chen, T.; Yao, Y. Recent development of pillar n arene-based amphiphiles. *Chin. Chem. Lett.* **2021**, *32* (4), 1267.

(26) Wu, Y.; Zhou, J.; Li, E.; Wang, M.; Jie, K.; Zhu, H.; Huang, F. Selective Separation of Methylfuran and Dimethylfuran by Non-

porous Adaptive Crystals of Pillararenes. *J. Am. Chem. Soc.* **2020**, *142* (46), 19722.
(27) Wang, H.; Jin, Y.; Sun, N.; Zhang, W.; Jiang, J. Post−synthetic modification of porous organic cages. *Chem. Soc. Rev.* **2021**, *50* (16), 8874.
(28) Hasell, T.; Cooper, A. I. Porous Organic Cages: Soluble, Modular and Molecular Pores. *Nat. Rev. Mater.* **2016**, *1* (9), 16053.
(29) Yang, X.; Ullah, Z.; Stoddart, J. F.; Yavuz, C. T. Porous Organic Cages. *Chem. Rev.* **2023**, *123*, 4602.
(30) Chakraborty, D.; Mukherjee, P. S. Recent trends in organic cage synthesis: push towards water-soluble organic cages. *Chem. Commun.* **2022**, *58* (37), 5558.
(31) Acharyya, K.; Mukherjee, P. S. Organic Imine Cages: Molecular Marriage and Applications. *Angew. Chem. Int. Ed.* **2019**, *58* (26), 8640.
(32) Mastalerz, M. Porous Shape-Persistent Organic Cage Compounds of Different Size, Geometry, and Function. *Acc. Chem. Res.* **2018**, *51* (10), 2411.
(33) Montà-González, G.; Sancenón, F.; Martínez-Máñez, R.; Martí-Centelles, V. J. C. R. Purely covalent molecular cages and containers for guest encapsulation. *Chem. Rev.* **2022**, *122* (16), 13636.
(34) Saha, R.; Mondal, B.; Mukherjee, P. S. Molecular Cavity for Catalysis and Formation of Metal Nanoparticles for Use in Catalysis. *Chem. Rev.* **2022**, *122* (14), 12244.
(35) Egleston, B. D.; Brand, M. C.; Greenwell, F.; Briggs, M. E.; James, S. L.; Cooper, A. I.; Crawford, D. E.; Greenaway, R. L. Continuous and scalable synthesis of a porous organic cage by twin screw extrusion (TSE). *Chem. Sci.* **2020**, *11* (25), 6582.
(36) Xu, T.; Wu, B.; Hou, L.; Zhu, Y.; Sheng, F.; Zhao, Z.; Dong, Y.; Liu, J.; Ye, B.; Li, X.; Ge, L.; Wang, H.; Xu, T. Highly Ion-Permselective Porous Organic Cage Membranes with Hierarchical Channels. *J. Am. Chem. Soc.* **2022**, *144* (23), 10220.
(37) Alimi, L. O.; Fang, F.; Moosa, B.; Ding, Y.; Khashab, N. M. Vapor-Triggered Mechanical Actuation in Polymer Composite Films Based on Crystalline Organic Cages. *Angew. Chem. Int. Ed.* **2022**, *61* (43), No. e202212596.
(38) He, A.; Jiang, Z.; Wu, Y.; Hussain, H.; Rawle, J.; Briggs, M. E.; Little, M. A.; Livingston, A. G.; Cooper, A. I. A smart and responsive crystalline porous organic cage membrane with switchable pore apertures for graded molecular sieving. *Nat. Mater.* **2022**, *21* (4), 463.
(39) Martinez-Ahumada, E.; He, D.; Berryman, V.; Lopez-Olvera, A.; Hernandez, M.; Jancik, V.; Martis, V.; Vera, M. A.; Lima, E.; Parker, D. J.; Cooper, A. I.; Ibarra, I. A.; Liu, M. SO2 Capture Using Porous Organic Cages. *Angew. Chem. Int. Ed.* **2021**, *60* (32), 17556.
(40) Wang, W.; Su, K.; Yuan, D. Porous organic cages for gas separations. *Mater. Chem. Front.* **2023**, *7* (21), 5247.
(41) Chen, L.; Reiss, P. S.; Chong, S. Y.; Holden, D.; Jelfs, K. E.; Hasell, T.; Little, M. A.; Kewley, A.; Briggs, M. E.; Stephenson, A.; Thomas, K. M.; Armstrong, J. A.; Bell, J.; Busto, J.; Noel, R.; Liu, J.; Strachan, D. M.; Thallapally, P. K.; Cooper, A. I. Separation of Rare Gases and Chiral Molecules by Selective Binding in Porous Organic Cages. *Nat. Mater.* **2014**, *13* (10), 954.
(42) Bhandari, P.; Mukherjee, P. S. Covalent Organic Cages in Catalysis. *ACS Catal.* **2023**, *13* (9), 6126.
(43) Hu, D.; Zhang, J.; Liu, M. Recent advances in the applications of porous organic cages. *Chem. Commun.* **2022**, *58* (81), 11333.
(44) Galan, A.; Ballester, P. Stabilization of Reactive Species by Supramolecular Encapsulation. *Chem. Soc. Rev.* **2016**, *45* (6), 1720.
(45) Gunawardana, V. W. L. W.; Ward, C.; Wang, H.; Holbrook, J. H.; Sekera, E. R.; Cui, H.; Hummon, A. B.; Badjic, J. D. Crystalline Nanoparticles of Water-Soluble Covalent Basket Cages (CBCs) for Encapsulation of Anticancer Drugs. *Angew. Chem. Int. Ed.* **2023**, *62*, No. e202306722.
(46) Jiao, T.; Qu, H.; Tong, L.; Cao, X.; Li, H. A Self-Assembled Homochiral Radical Cage with Paramagnetic Behaviors. *Angew. Chem. Int. Ed.* **2021**, *60* (18), 9852.
(47) Zhang, C.; Wang, Q.; Long, H.; Zhang, W. A highly C70 selective shape-persistent rectangular prism constructed through one-step alkyne metathesis. *J. Am. Chem. Soc.* **2011**, *133* (51), 20995.
(48) Liu, X.; Zhu, G.; He, D.; Gu, L.; Shen, P.; Cui, G.; Wang, S.; Shi, Z.; Miyajima, D.; Wang, S.; Zhang, S. Guest-Mediated Hierarchical Self-Assembly of Dissymmetric Organic Cages to Form Supramolecular Ferroelectrics. *CCS Chem.* **2022**, *4* (7), 2420.
(49) Cheng, L.; Tian, P.; Li, Q.; Li, A.; Cao, L. Stabilization and Multiple-Responsive Recognition of Natural Base Pairs in Water by a Cationic Cage. *CCS Chem.* **2022**, *4* (9), 2914.
(50) Luo, D.; He, Y.; Tian, J.; Sessler, J. L.; Chi, X. Reversible Iodine Capture by Nonporous Adaptive Crystals of a Bipyridine Cage. *J. Am. Chem. Soc.* **2022**, *144* (1), 113.
(51) Mukhopadhyay, R. D.; Kim, Y.; Koo, J.; Kim, K. Porphyrin Boxes. *Acc. Chem. Res.* **2018**, *51* (11), 2730.
(52) Yu, C.; Jin, Y.; Zhang, W. Shape-Persistent Arylene Ethynylene Organic Hosts for Fullerenes. *Chem. Rec.* **2015**, *15* (1), 97.
(53) Moosa, B.; Alimi, L. O.; Shkurenko, A.; Fakim, A.; Bhatt, P. M.; Zhang, G.; Eddaoudi, M.; Khashab, N. M. A Polymorphic Azobenzene Cage for Energy-Efficient and Highly Selective p-Xylene Separation. *Angew. Chem. Int. Ed.* **2020**, *59* (48), 21367.
(54) Ding, Y.; Alimi, L. O.; Moosa, B.; Maaliki, C.; Jacquemin, J.; Huang, F.; Khashab, N. M. Selective adsorptive separation of cyclohexane over benzene using thienothiophene cages. *Chem. Sci.* **2021**, *12* (14), 5315.
(55) Zhao, X.; Liu, Y.; Zhang, Z.-Y.; Wang, Y.; Jia, X.; Li, C. One-Pot and Shape-Controlled Synthesis of Organic Cages. *Angew. Chem. Int. Ed.* **2021**, *60* (33), 17904.
(56) Hasell, T.; Miklitz, M.; Stephenson, A.; Little, M. A.; Chong, S. Y.; Clowes, R.; Chen, L. J.; Holden, D.; Tribello, G. A.; Jelfs, K. E.; Cooper, A. I. Porous Organic Cages for Sulfur Hexafluoride Separation. *J. Am. Chem. Soc.* **2016**, *138* (5), 1653.
(57) Tian, K.; Elbert, S. M.; Hu, X.-Y.; Kirschbaum, T.; Zhang, W.-S.; Rominger, F.; Schroeder, R. R.; Mastalerz, M. Highly Selective Adsorption of Perfluorinated Greenhouse Gases by Porous Organic Cages. *Adv. Mater.* **2022**, *34* (31), 2202290.
(58) Liu, M.; Zhang, L.; Little, M. A.; Kapil, V.; Ceriotti, M.; Yang, S.; Ding, L.; Holden, D. L.; Balderas-Xicohtencatl, R.; He, D.; Clowes, R.; Chong, S. Y.; Schutz, G.; Chen, L.; Hirscher, M.; Cooper, A. I. Barely Porous Organic Cages for Hydrogen Isotope Separation. *Science* **2019**, *366* (6465), 613.
(59) Mitra, T.; Jelfs, K. E.; Schmidtmann, M.; Ahmed, A.; Chong, S. Y.; Adams, D. J.; Cooper, A. I. Molecular shape sorting using molecular organic cages. *Nat. Chem.* **2013**, *5* (4), 276.
(60) Fang, S.; Wang, M.; Wu, Y.; Guo, Q.-H.; Li, E.; Li, H.; Huang, F. Cagearenes: synthesis, characterization, and application for programmed vapour release. *Chem. Sci.* **2022**, *13* (21), 6254.
(61) Moosa, B.; Alimi, L. O.; Shkurenko, A.; Fakim, A.; Bhatt, P. M.; Zhang, G.; Eddaoudi, M.; Khashab, N. M. A Polymorphic Azobenzene Cage for Energy-Efficient and Highly Selectivep-Xylene Separation. *Angew. Chem. Int. Ed.* **2020**, *59* (48), 21367.
(62) Kobayashi, K.; Yamanaka, M. Self-Assembled Capsules based on Tetrafunctionalized Calix[4]resorcinarene Cavitands. *Chem. Soc. Rev.* **2015**, *44* (2), 449.
(63) Yang, M.; Qiu, F.; El-Sayed, M. E.; Wang, W.; Du, S.; Su, K.; Yuan, D. Water-stable hydrazone-linked porous organic cages. *Chem. Sci.* **2021**, *12* (40), 13307.
(64) Su, K.; Wang, W.; Du, S.; Ji, C.; Zhou, M.; Yuan, D. Reticular Chemistry in the Construction of Porous Organic Cages. *J. Am. Chem. Soc.* **2020**, *142* (42), 18060.
(65) Gao, F.; Luo, C.; Wang, X.; Zhan, C.; Li, Y.; Li, Y.; Meng, Q.; Yang, M.; Su, K.; Yuan, D.; Zhu, R.; Zhao, Q. Porous Organic Cage Induced Spontaneous Restructuring of Buried Interface Toward High-Performance Perovskite Photovoltaic. *Adv. Funct. Mater.* **2023**, *33* (17), 2211900.
(66) Xu, N.; Su, K.; El-Sayed, E.-S. M.; Ju, Z.; Yuan, D. Chiral proline-substituted porous organic cages in asymmetric organo-catalysis. *Chem. Sci.* **2022**, *13* (12), 3582.
(67) Yang, M.; Wang, W.; Su, K.; Yuan, D. Dimeric Calix 4 resorcinarene-based Porous Organic Cages for CO2/CH4 Separation. *Chem. Res. Chin. Univ.* **2022**, *38* (2), 428.

https://doi.org/10.1021/cbe.3c00099
Chem Bio Eng. 2024, 1, 171−178

(68) Zhang, X.; Su, K.; Mohamed, A. G. A.; Liu, C.; Sun, Q.; Yuan, D.; Wang, Y.; Xue, W.; Wang, Y. Photo-assisted charge/discharge Li-organic battery with a charge-separated and redox-active C_{60}@porous organic cage cathode. *Energy Environ. Sci.* **2022**, *15* (2), 780.
(69) Su, K.; Wang, W.; Du, S.; Ji, C.; Yuan, D. Efficient ethylene purification by a robust ethane-trapping porous organic cage. *Nat. Commun.* **2021**, *12*, 3703.
(70) Yang, M.; Chen, X.; Xie, Y.; El-Sayed, E.-S. M.; Xu, N.; Wang, W.; Su, K.; Yuan, D. Post-synthetic metalation of organic cage for enhanced porosity and catalytic performance. *Sci. China Chem.* **2023**, *66* (6), 1763.
(71) Grajda, M.; Wierzbicki, M.; Cmoch, P.; Szumna, A. Inherently Chiral Iminoresorcinarenes through Regioselective Unidirectional Tautomerization. *J. Org. Chem.* **2013**, *78* (22), 11597.
(72) Kirkpatrick, S.; Gelatt, C. D.; Vecchi, M. P. Optimization By Simulated Annealing. *Science* **1983**, *220* (4598), 671.
(73) Kuehne, T. D.; Iannuzzi, M.; Del Ben, M.; Rybkin, V. V.; Seewald, P.; Stein, F.; Laino, T.; Khaliullin, R. Z.; Schutt, O.; Schiffmann, F.; Golze, D.; Wilhelm, J.; Chulkov, S.; Bani-Hashemian, M. H.; Weber, V.; Borstnik, U.; Taillefumier, M.; Jakobovits, A. S.; Lazzaro, A.; Pabst, H.; Mueller, T.; Schade, R.; Guidon, M.; Andermatt, S.; Holmberg, N.; Schenter, G. K.; Hehn, A.; Bussy, A.; Belleflamme, F.; Tabacchi, G.; Gloss, A.; Lass, M.; Bethune, I.; Mundy, C. J.; Plessl, C.; Watkins, M.; VandeVondele, J.; Krack, M.; Hutter, J. CP2K: An electronic structure and molecular dynamics software package - Quickstep: Efficient and accurate electronic structure calculations. *J. Chem. Phys.* **2020**, *152* (19), 194103.
(74) Lu, T.; Chen, F. Multiwfn: A multifunctional wavefunction analyzer. *J. Comput. Chem.* **2012**, *33* (5), 580.
(75) Bannwarth, C.; Caldeweyher, E.; Ehlert, S.; Hansen, A.; Pracht, P.; Seibert, J.; Spicher, S.; Grimme, S. Extendedtight-bindingquantum chemistry methods. *WIREs Comput. Mol. Sci.* **2021**, *11* (2), No. e1493.
(76) Grimme, S.; Antony, J.; Ehrlich, S.; Krieg, H. A consistent and accurate ab initio parametrization of density functional dispersion correction (DFT-D) for the 94 elements H-Pu. *J. Chem. Phys.* **2010**, *132* (15), 154104.
(77) Spicher, S.; Bursch, M.; Grimme, S. Efficient Calculation of Small Molecule Binding in Metal-Organic Frameworks and Porous Organic Cages. *J. Phys. Chem. C* **2020**, *124* (50), 27529.
(78) Pracht, P.; Bohle, F.; Grimme, S. Automated exploration of the low-energy chemical space with fast quantum chemical methods. *Phys. Chem. Chem. Phys.* **2020**, *22* (14), 7169.

https://doi.org/10.1021/cbe.3c00099
Chem Bio Eng. 2024, 1, 171−178